Energy 316 (2025) 134511

Contents lists available at ScienceDirect

Energy

journal homepage: www.elsevier.com/locate/energy

Unlocking the flexibilities of data centers for smart grid services: Optimal dispatch and design of energy storage systems under progressive loading

Yingbo Zhang [a], Hong Tang [a], Hangxin Li [a,**], Shengwei Wang [a,b,*]

[a] Department of Building Environment and Energy Engineering, The Hong Kong Polytechnic University, Hong Kong
[b] Research Institute for Smart Energy, The Hong Kong Polytechnic University, Hong Kong

ARTICLE INFO

Handling editor: X Zhao

Keywords:
Data center
Progressive loading
Energy storage system
Design optimization
Grid flexibility services
Optimal dispatch

ABSTRACT

As the backbone of the digital world, data centers have placed great stress on the power grids, labeled “electricity hogs”. However, this challenge also presents a unique opportunity for data centers to become key contributors to grid stability by offering flexible services. By leveraging this opportunity, data centers can potentially reduce their energy costs, creating a win-win situation. This study pioneers utilizing the surplus capacity of energy storage systems for emergencies in data centers to provide grid flexibility services under progressive loading conditions. Two optimization problems are formulated: one for the optimal dispatch of energy storage capacity and another for design optimization of storage systems. The objective of optimal dispatch is to minimize the electricity cost, by efficiently allocating battery and cold storage capacities. The design optimization aims to minimize life-cycle costs, including investments and operational cost savings, under typical loading conditions and electricity markets. The study considers two typical electricity markets (Guangdong electricity market and CAISO electricity market) and four investment scenarios for energy storage systems. The impacts of discount rates and battery prices on the life-cycle economic benefits are also analyzed comprehensively. Results show significant economic benefits for data centers in providing grid flexibility services. Over the lifetime, the battery storage can achieve economic benefits of $1.6 million, which is 1.29 times its total investment. The cold storage can achieve economic benefits of $0.35 million, which is 2.39 times its total investment.

1. Introduction

1.1. Background and motivation

Spearheaded by the proliferation of technologies such as generative AI, 5G, and augmented reality, the demand for data center capacity across the globe has increased dramatically over the past decade. In 2021, global data centers consumed 220–320 TWh of electricity [1], representing 1 %–1.5 % of the world’s total electricity usage [2]. This significant energy demand has cast data centers ‘electricity hogs’, placing considerable strain on the power grid. However, this challenge is accompanied by a unique opportunity: data centers possess the potential to act as stabilizing agents for the grid by providing ancillary services. Furthermore, this opportunity allows data centers to potentially reduce their energy costs and even generate revenue, creating a win-win situation.

1.2. Opportunities for data centers interacting with the power grid

Data centers have the potential to play a significant role in the future energy landscape by actively participating in grid interactions and supporting the transition to a more sustainable and resilient power system. Current research on the interaction of data centers and power grid falls into the following categories.

i) Renewable Energy Integration [3,4]. Data centers can integrate renewable energy sources, such as solar or wind, into their operations. They can consume renewable energy directly or even generate excess energy to feed back into the grid [5,6]. He et al. [7] conducted an analysis of the power supply systems in data centers utilizing various renewable energy combinations. Their findings indicate that a hybrid renewable power system can achieve a maximum renewable energy penetration of 28.31 %. Han et al. [8] introduced a business model for shared energy

* Corresponding author. Department of Building Environment and Energy Engineering, The Hong Kong Polytechnic University, Hong Kong.
** Corresponding author.
E-mail addresses: hangxin.li@polyu.edu.hk (H. Li), beswwang@polyu.edu.hk (S. Wang).

https://doi.org/10.1016/j.energy.2025.134511
Received 7 August 2024; Received in revised form 19 December 2024; Accepted 11 January 2025
Available online 11 January 2025
0360-5442/

storage in data center clusters, taking into account the uncertainties associated with renewable energy. This model can reduce the daily operational costs of data centers by 26.36 %.

ii) Demand response resources. As Lawrence Berkeley National Laboratory (LBNL) reported "data centers are excellent candidates with great potential for smart grid demand response" [9]. There are some potential demand-side resources to participate in load shedding and load-shifting in data centers.
   - *IT equipment.* Servers can adjust their energy consumption through power management systems, such as Dynamic Voltage/Frequency Scaling (DVFS) [10] and power-capping [11]. Chen et al. [12] reported that participating in smart grid demand response programs, i.e., regulation services and frequency control, can reduce data center electricity costs by up to 68.3 % while meeting the service level agreements (SLAs) for quality of service (QoS). Zhang et al. [13] demonstrate that data centers can save their electricity costs by 10 % while abiding by all the QoS constraints in a real-world scenario through workload scheduling and CPU power limiting. On the other hand, data centers have delay-tolerant workloads, which can be shifted in time in response to electricity prices or other grid requests. Hu et al. [14] investigate cost-efficient workload scheduling, including both the non-elastic interactive workload and the elastic batch workload, for the coordination between the cloud service provider with geo-distributed data centers and smart grids. Their results show that the cost of smart grids can be significantly reduced, by up to 20 %, and the load variations of smart grids can be well smoothed simultaneously, by scheduling computing workloads.
   - *Cooling system.* Data centers can operate under a broad range of temperatures [15], which will result in a large range of cooling energy. Ghatikar et al. [16] made a field test on the ability of data center cooling systems to participate in demand response. Their results show that the response time of activating/deactivating redundant chillers/Computer Room Air Conditioner units (CRACs) is 2–8 min. Fu et al. [17] proposed a synergistic control strategy by adjusting the frequency of the servers and the chilled water supply temperature setpoint simultaneously to track the regulation signal from the electrical market. They concluded that the proposed synergistic control strategy could provide an extra regulation capacity of 3 % of the design power when chillers are activated, compared with a server-only control strategy.
   - *Back-up system.* Back-up generators powered by diesel or natural gas are usually configured to start in two to 4 s after a utility outage or voltage fluctuation [18]. However, utilizing backup generators for in-demand response programs is not environmentally friendly [17].

iii) Energy storage integration: Data centers can integrate energy storage systems, such as batteries, to store excess energy when demand is low and use it during peak times. This can help to reduce strain on the grid during periods of high demand. Zhang et al. [19] proposed a strategy to leverage thermal storage to cut the electricity bill for cooling, and found that the electricity bill for cooling can be reduced by 15.8 %–20.8 % under different CPU utilization levels. Yang et al. [20] found that data center micro-grid tie-line power fluctuations can be effectively regulated by UPS battery group dynamical management. Aksanli analyzed the economic feasibility of using energy storage devices in data centers to reduce their maximum power demand. Guo et al. [21] studied the co-planning problem of networked Internet data centers and battery energy storage systems in a smart grid system. Their results show that the system's quality-of-service, economics, and reliability can be significantly enhanced, by coordinately planning the data centers' and battery energy storage systems' locations and sizes.

1.3. Progressive loading and surplus energy storage in data centers

Data centers are specifically engineered to meet strict reliability standards to ensure continuous uptime. The Uptime Institute has established two high-availability classes for data centers: Tier III (99.982 % availability) and Tier IV (99.995 % availability) [17]. These classifications indicate the level of reliability and uptime that data centers are designed to achieve. To maintain this level of reliability, typical emergency designs for data centers include 15-min cold energy storage and 15-min battery storage systems corresponding to the design 100 % IT load [22]. These systems are crucial for ensuring uninterrupted power supply in the event of an emergency or power outage.

On the other hand, most data centers work at partial loads throughout most of their working lifetime, instead of at full 100 % IT load [23,24]. During the initial years (1–8 years), the IT load generally shows a gradual increase, eventually stabilizing at around 60 % of the design IT load for the subsequent 8–15 years [25]. This indicates that there is unused energy storage capacity in emergency systems that can be utilized to interact with the power grid, which is named surplus capacity. This is a significant opportunity for data centers to leverage the surplus energy storage capacity to provide grid services without requiring additional investments.

1.4. Identified research gaps and key innovations

Previous studies have put forward various solutions for data centers to interact with the power grid. However, to our best knowledge, no studies address the interaction with the power grid using surplus energy storage capacity in emergency systems in data centers, particularly in the context of progressive IT loading. By utilizing surplus energy storage capacity in emergency systems, data centers can provide multiple grid flexibility services without compromising their reliability since the capacity is in an unused state.

This pioneering study focuses on the optimal dispatch and design of energy storage systems for emergencies in data centers, particularly in the context of progressive IT loading. *Firstly*, the surplus capacities for both thermal energy storage (TES) and electrical energy storage (EES) systems are identified, based on a typical progressive loading profile. The potential for TES and EES to provide grid flexibility services is also identified according to their response characteristics. *Secondly*, the study formulates a mixed integer linear problem (MILP) or quadratic programming problem (MIQP) with the objective of minimizing electricity costs. This involves the strategic allocation of surplus capacities to provide a suite of flexible services. *Thirdly*, two typical electricity markets (Guangdong electricity market in China and the California Independent System Operator (CAISO) electricity market in the United States) and four investment scenarios for energy storage systems are considered. The optimal design scenario is determined with the aim of minimizing the life-cycle costs under typical loading conditions and electricity markets. *Lastly*, the impacts of discount rates and battery prices on the life-cycle economic benefits of EES and TES are also comprehensively discussed. The results provide valuable insights into the optimal dispatch and design of energy storage systems in data centers and the meaningful reference for the development of next-generation data centers that can engage grid interactions, contributing to the carbon neutrality of power systems.

2. Formulation of optimization problems considering effective use of surplus capacity of storage systems in flexibility markets

2.1. Typical progressive IT loading and surplus capacity

Fig. 1 shows dynamic IT load increases in data centers over their operational lifetime [25]. Initially, the initial load is estimated to be approximately 20 % of the design capacity, progressively increasing in stages to ultimately reach around 60 % of the design capacity. The load

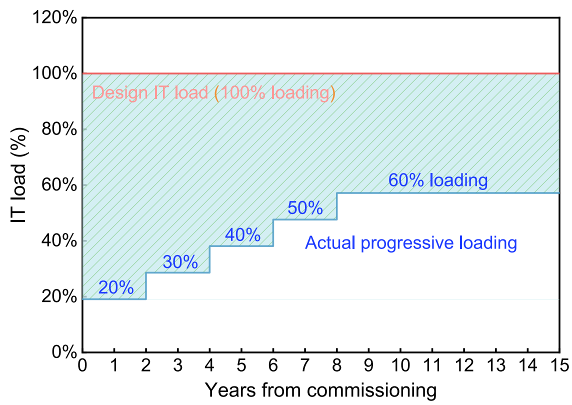

Fig. 1. Typical progressive IT loading profile throughout the lifetime.

increase follows several stages: 20 % in the initial stage, 30 % in the second stage, 40 % in the third stage, 50 % in the fourth stage, and ultimately 60 % in the fifth stage.

Typical emergency designs for data centers include 15-min cold energy storage and 15-min battery storage systems, designed to support 100 % of the IT load [22]. These systems are essential for ensuring uninterrupted power supply in the event of an emergency or power outage. In the context of progressive loading, there is unused energy storage capacity in emergency systems, which is named surplus capacity. The surplus energy storage can be flexibly scheduled at each stage throughout the data center's lifecycle, without compromising the reliability of the data center. Data centers can leverage the surplus energy storage capacity to provide grid services without requiring additional investments to stabilize the grid and generate revenues, creating a win-win situation.

2.2. Typical electricity markets and flexibility services

Pricing mechanisms vary across countries or regions that are managed by different independent system operators. For instance, the electricity market in the United States, specifically CAISO, is managed by an independent system operator and operates using a joint market model, allowing for the simultaneous trading of energy and ancillary services. In contrast, China's Time of Use (ToU) electricity market utilizes a time-based pricing system, which leverages differential electricity prices during different periods to encourage users to shift their electricity consumption from peak hours, thereby alleviating peak load pressure on the power system.

This study selects these two electricity markets as backgrounds to analyze the potential benefits of the effective use of the surplus capacity in energy storage systems in data centers. One is the CAISO (California Independent System Operator) electricity market in the United States, which offers various services for demand-side participants. The historical data in 2020 from CAISO's energy markets is obtained from the official website [26].

The other electricity market is the Time of Use (ToU) electricity market in Guangdong Province, China. In a typical three-period ToU tariff, electricity prices are divided into peak, flat, and valley prices to incentivize users to shift their demand from peak hours to off-peak hours, thereby alleviating the burden of peak power generation for the power system [27]. The data for the Time of Use (ToU) electricity market in Guangdong Province is obtained from the official website [28], and the rewards of grid services in China's electricity market are obtained from Ref. [29].

Demand-side flexibility involves the capacity to modify consumption patterns while engaging with the power grid. Energy flexibility in data centers for the grid includes energy arbitrage and ancillary services, such as frequency regulation and spinning reserve. Energy arbitrage involves leveraging flexible resources to transfer energy use from peak-price times to off-peak times, resulting in economic benefits. Ancillary services require flexible resources to respond rapidly to ensure a short-term balance in power distribution. For instance, in the process of frequency regulation, system authorities measure the power imbalance as the area control error (ACE), which is then converted into normalized automatic generation control (AGC) signals that vary from −1 to 1. These signals are continuously transmitted to service providers at second intervals. The spinning reserve requires resources to be synchronized to the grid and respond within 10 min. Participants on the demand side offering spinning reserve service must be capable of swiftly curtailing their load for a short period upon an urgent request from the power grid.

2.3. Formulation for optimizing dispatching energy flexibilities

Fig. 2 illustrates the flowchart of dispatch optimization of surplus energy storage in data centers. The optimization objective is to minimize operational costs, which involve energy arbitrage and revenues from frequency regulation and spinning reserve services. Each dispatch optimization has a 24-h horizon with a time step of 1 h. Optimization variables include the hourly rates of discharging and charging for the battery and TES tank, along with the hourly capacities allocated for ancillary services. The optimization objective of dispatch optimization of surplus energy storage in data centers is presented as follows.

$$\text{Min} \sum_{k\in T}\left(\pi_k^E P_k^E h - \pi_k^{SR} Cap_k^{SR} - \pi_k^{FR} Cap_k^{FR}\right) \forall\, k \in [1, 24] \tag{1}$$

where, $\pi_k^E, \pi_k^{SR}, \pi_k^{FR}$ are the energy price, the revenues for providing spinning reserve service and frequency regulation service at the hour k. P_k^E is the total energy consumption at the hour k. Cap_k^{SR} is the provided spinning reserve capacity at the hour k. Cap_k^{FR} is the provided frequency regulation capacity at the hour k.

2.3.1. Optimal dispatch strategy of electrical energy storage (EES)

In addition to leveraging energy arbitrage, batteries are perfectly suited for providing frequency regulation and spinning reserve services due to their fast response speed. The optimization objective for dispatching surplus capacity in EES is presented in Equation (2). Formulations (3)–(4) show operating constraints associated with scheduling capacity in market services. Notably, it is assumed that frequency regulation has an ideally neutral effect on hourly energy consumption (kWh). This assumption is based on the design of the regulation signal, which is intended to average out to zero over a specified timeframe (e.g., 1 h), following the guidelines set by the Independent System Operator (ISO) [30]. The defined minimum and maximum values of the state of charge of batteries are presented in Formulation (7). Establishing appropriate upper and lower boundaries can significantly mitigate batteries degradation.

The battery's operational depth of discharge (DoD) has a significant impact on its lifecycle. Here, we limit the DoD to below 60 %, as exceeding this threshold can lead to a shorter lifespan for the battery. When DoD is set at 60 %, the losses incurred from participating in grid regulation services throughout the life cycle are nearly equivalent to the losses experienced when leaving the energy storage systems unused [31, 32].

$$P_k^E = P_{EES,k}^{\wedge} - P_{EES,k}^{\vee} \tag{2}$$

$$P_{EES,k}^{\wedge} + Cap_{EES,k}^{FR} \le P_{EES,rated} \tag{3}$$

$$-P_{EES,k}^{\vee} - Cap_{EES,k}^{FR} - Cap_{EES,k}^{SP} \ge -P_{EES,rated} \tag{4}$$

$$P_{EES,rated} = E_{EES,rated} \big/ r_{ep} \tag{5}$$

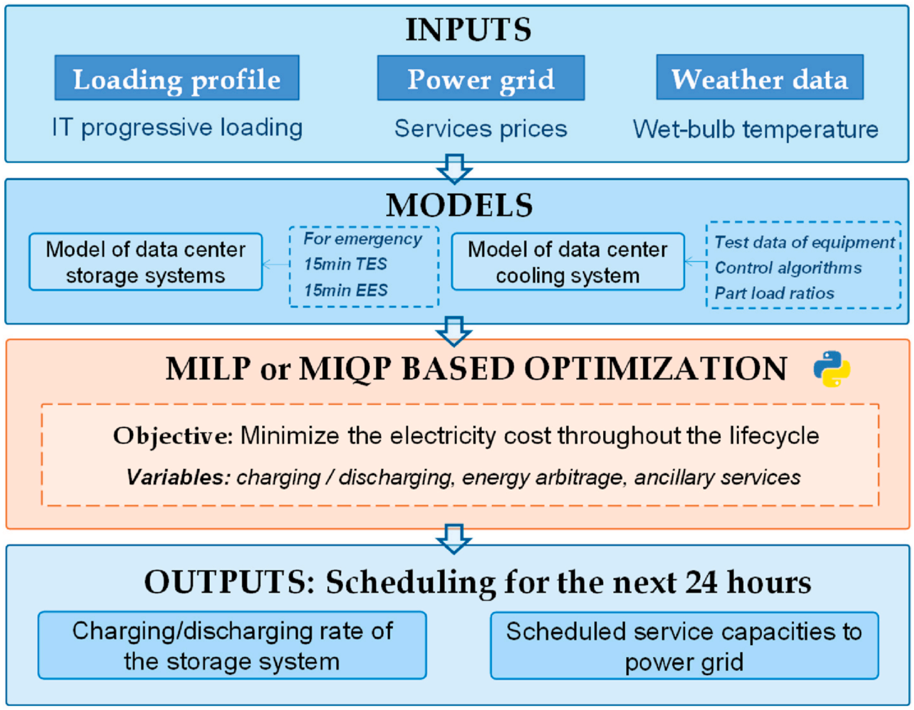

Fig. 2. Flowchart of dispatch optimization of surplus energy storage in data centers.

$$SOC_{EES,k+1} = SOC_{EES,k} + \left(P^{\wedge}_{EES,k}\eta_{EES} - P^{\vee}_{EES,k} \Big/ \eta_{EES}\right) \Big/ E_{EES,rated} \tag{6}$$

$$\underline{SOC}_{EES} \le SOC_{EES,k} \le \overline{SOC}_{EES} \tag{7}$$

where, $P^{\wedge}_{EES,k}$ and $P^{\vee}_{EES,k}$ are the charging and discharging states of batteries at the hour k, respectively. When the storage is being discharged at $P^{\vee}_{EES,k}$, the charging power $P^{\wedge}_{EES,k}$ is equal to 0 and vice versa. $P_{EES,rated}$ is the rated charging/discharging rate. $E_{EES,rated}$ is rated battery capacity. r_{ep} is energy to power ratio. $SOC_{EES,k}$ is the state of charge at the hour k. η_{EES} is the battery charging/discharging efficiency. $\underline{SOC}_{EES}$ and $\overline{SOC}_{EES}$ are lower and upper of the battery, 0.2 and 0.8, respectively.

2.3.2. Optimal dispatch strategy of thermal energy storage (TES)

Cooling systems integrated with TES typically have a slower response speed in terms of power adjustment (minutes to hours). Therefore, TES cannot provide frequency regulation services to precisely track the grid control signals, which require faster response speed in the timescale of seconds. However, TES has the capability to offer significant power reduction and shifting capacity within hours. In the optimization of the dispatch of TES capacity, only spinning reserve service and energy arbitrage are taken into account. Equation (8) presents the optimization objective for the dispatching surplus capacity in TES. Formulations (12)–(14) show the operating constraints associated with the flexible scheduling of TES capacity.

$$P^{E}_{k} = \frac{Q_{dem,k} + Q_{TES,k}}{COS\ P_k} \tag{8}$$

$$COS\ P_k = f\left(PLR_k, T_{wet,k}\right) \tag{9}$$

$$PLR_k = \frac{Q_{dem,k} + Q_{TES,k}}{N_{op} * Q_{EC,rated}} \tag{10}$$

$$Q_{store,k} = \eta_{TES} Q_{store,k-1} + Q_{TES,k} \tag{11}$$

$$0.3 \le PLR_k \le 1 \tag{12}$$

$$\left|Q_{TES,k}\right| \le Q_{TES,rated} \tag{13}$$

$$0 \le Q_{store,k} \le Q_{TES,rated} \tag{14}$$

$$0 \le Cap^{SP}_{TES,k} \le \min\left(Q_{store,k}, Q_{EC,k}, Q_{TES,rated} + Q_{TES,k}\right) \Big/ COS\ P_k \tag{15}$$

where, $Q_{dem,k}$ is the cooling demand at the hour k. $Q_{TES,k}$ is the charging/discharging of TES at the hour k. $COS\ P_k$ is the coefficient of performance of the cooling system at the hour k. PLR_k is the part load ratio of the cooling system. $T_{wet,k}$ is the wet-bulb temperature. $Q_{store,k}$ is the thermal energy storage at the hour k. $Q_{EC,rated}$ is the rated cooling capacity of the electric chiller. η_{TES} is TES tank's storage efficiency. N_{op} is the quantity of chillers in operation.

2.4. Description of investment scenarios for energy storage systems

Fig. 3 shows the energy storage profile of the baseline scenario and design scenarios 1–4 throughout the lifetime. In the baseline scenario, the energy storage system for emergencies is a one-time investment and

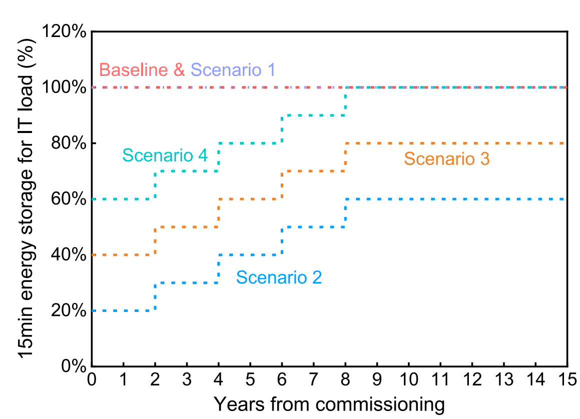

Fig. 3. Surplus capacities of different scenarios throughout the lifecycle.

does not participate in the grid. *In Scenario 1*, the energy storage system for emergencies is a one-time investment and provides auxiliary services to the grid throughout the data center's lifecycle, utilizing the surplus energy storage capacity. *In Scenario 2*, the energy storage system for emergencies is a phased investment based on progressive IT loading. There is no additional dispatchable capacity to provide auxiliary services to the grid. *In Scenario 3*, the energy storage system for emergencies is a phased investment based on progressive IT loading, with an additional 20 % capacity corresponding to the progressive loading. The extra 20 % capacity at each stage can be flexibly scheduled to provide auxiliary services. *In Scenario 4*, the energy storage system for emergencies is a phased investment based on progressive IT loading, with an additional 40 % capacity corresponding to the progressive loading. The extra 40 % capacity at each stage can be flexibly scheduled to provide auxiliary services.

2.5. Formulation for optimizing storage system design in data centers

Typically, life-cycle economic analysis is used as an effective means to determine the most cost-effective solution from multiple options by comparing their economic benefits over their lifetime. The objective of optimizing storage system design is to minimize the life-cycle cost.

$$\text{Minimize } LCC = C_{INV} + C_{REP} + \sum_{i=1}^{L} \frac{(C_{O\&M,i} - Rev_i)}{(1+r)^i} \tag{16}$$

where, LCC is the life-cycle cost, C_{INV} is the total investment cost throughout the lifetime, C_{REP} is the total replacement cost throughout the lifetime, $C_{O\&M,i}$ is the maintenance cost at ith year, Rev_i is the total revenue at ith year, r is the discount rate. L is the lifetime. i is the ith year after the investment.

For electrical energy storage, the investment and replacement costs at ith year are given in Equations (17) and (18).

$$C_{INV,i} = \frac{C_{INV,0}}{(1+r)^i} * d \tag{17}$$

$$C_{REP,i} = \frac{C_{INV,0}}{(1+r)^i} * d \tag{18}$$

where, d is the annual decline rate of battery price.

For thermal energy storage, the investment cost at ith year is shown as follows.

$$C_{INV,i} = \frac{C_{INV,0}}{(1+r)^i} \tag{19}$$

Fig. 4 illustrates the schematic of the economic performance analysis of energy storage systems. The economic performance is assessed using the life-cycle cost (LCC) indicator, as shown in Equation (16). The investment costs include initial costs, operation and maintenance costs, and replacement costs. Economic benefits are maximized by leveraging multiple revenue streams through optimized dispatch strategies. Investment, operational costs and revenues are discounted over the data center's lifetime using an assumed discount rate. Additionally, the annual decline rate of battery price is considered in the economic analysis.

3. Description of energy storage and cooling systems in the referenced data center

3.1. Referenced data center and energy storage systems for emergency

In the referenced data center [33], the design IT load is 16800 kW. The standard design for both EES and TES is to provide enough electrical power or cooling energy to cover the design IT load for 15 min in case of an emergency [22]. Table 1 shows the specifications of EES and TES in the referenced data center.

Table 1
Specifications of energy storage systems in the referenced data center.

Thermal Energy Storage (TES)	
Design capacity	600 m^3
Capacity cost	31.8 $/kWh [34]
O&M cost/year	0.7 % of investment cost [35]
Design lifespan	20 years [34]
Energy storage efficiency	0.995 [36]
Electrical Energy Storage (EES)	
Design capacity	4200 kWh
Capacity cost	200 $/kWh [37]
O&M cost/year	0.5 % of investment cost [35]
Battery cycle (to end-of-life)	9000 [31]
Battery float lifespan	10 years [38]
Charging/discharging efficiency	0.95 [31]
Energy-to-Power ratio	2.8 [31]
Other parameters	
r (discount rate)	4 % [39]
d (annual decline rate of battery price)	5 % [37]

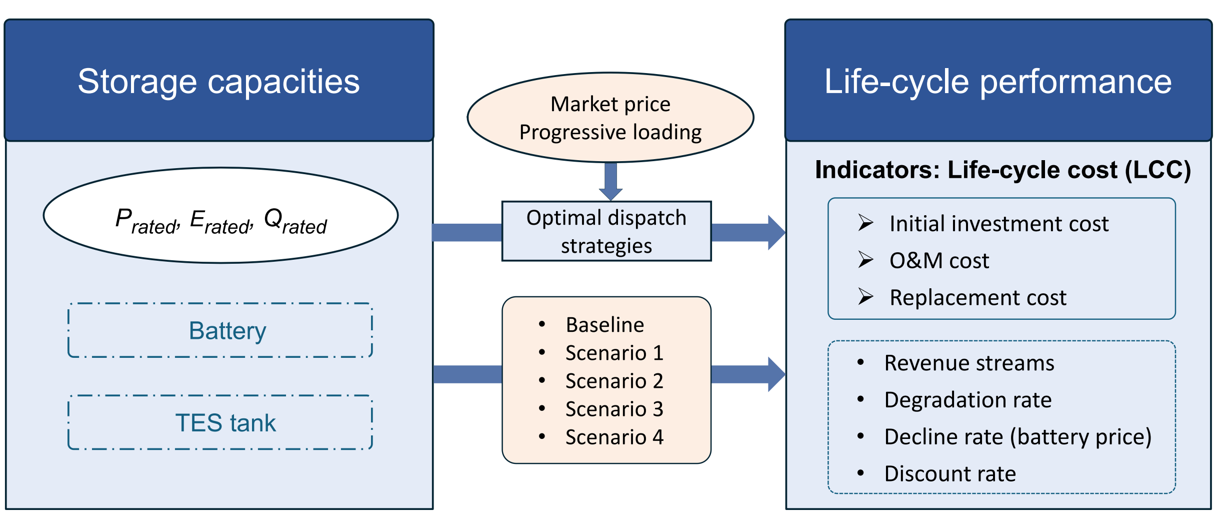

Fig. 4. The schematic of life-cycle economic analysis.

3.2. Specification of the cooling system in the referenced data center

The cooling system is a centralized cooling plant with multiple chillers and water-side economizers. Fig. 5 shows the schematic of the cooling system in the referenced data center. Fig. 6 shows the schematic of the cooling unit, which comprises an open cooling tower, a constant-speed cooling water pump, a heat exchanger, a chiller, and a variable-speed chilled water pump. Table 2 shows the specification of the cooling equipment of the cooling system. In addition, the cooling system has three cooling operation modes, which are free cooling mode, partial free cooling mode and mechanical cooling mode. A detailed explanation of the three operation modes can be found in Ref. [33].

3.3. Mathematical formulas and control algorithms

3.3.1. Chiller models

The chiller is modeled using Braun's method [40], involving two key variables: the load and the temperature difference between the leaving condenser and chilled water flows. Equation (20) represents the correlation between chiller power and these variables. Additionally, the chiller performance data is sourced from the manufacturer, Trane.

$$\frac{P_{ch}}{P_{des}} = a_0 + a_1X + a_2X^2 + a_3Y + a_4Y^2 + a_5XY \tag{20}$$

$$\mathrm{X} = \frac{\dot{Q}_e}{\dot{Q}_{des}} \tag{21}$$

$$\mathrm{Y} = \frac{(T_{cwr} - T_{chws})}{\Delta T_{des}} \tag{22}$$

where, X is the ratio of the chiller load to the design load. Y is the leaving water temperature difference divided by a design value. P_{ch} is the chiller power consumption and P_{des} is the power consumption at the design condition. The empirical coefficients in Equation (20) (a_0, a_1, a_2, a_3, a_4 *and* a_5) are based on the manufacturer's chiller performance data. Table 3 shows the parameters associated with the chiller model. The chiller model is validated and has a multiple R of 0.9911, an R^2 of 0.9823, and a standard error of 3.06 %. Additionally, this study assumes that the approach temperature of heat exchangers is 1.5 °C [41,42].

The chilled water supply temperature is maintained at 13 °C. This temperature (13 °C) is achieved through the use of chillers in both mechanical cooling mode and partial free cooling mode. In free cooling mode, this temperature (13 °C) is regulated by adjusting the rotational speed of the cooling tower fans.

3.3.2. Cooling tower models

The open cooling tower is modeled using the ε-NTU method [43]. According to Braun [40], air effectiveness(ε) can be obtained according to relationships for sensible heat exchangers, the number of transfer units, and the capacitance rate ratios. It is worth noting that the assumption of the Lewis number is one. The air effectiveness can be described by Equation (23).

$$\varepsilon_a = \frac{1 - \exp\left(-NTU(1 - m^*)\right)}{1 - m^* \exp\left(-NTU(1 - m^*)\right)} \tag{23}$$

where,

$$\mathrm{NTU} = \frac{h_D A_v V_{cell}}{m_a} \tag{24}$$

$$m^* = \frac{m_a C_s}{m_{w,i} C_{pw}} \tag{25}$$

The saturation-specific heat, C_s, can be calculated using inlet and outlet conditions along with psychrometric data, as shown in Equation (26).

$$C_s = \frac{h_{s,w,i} - h_{s,w,o}}{T_{w,i} - T_{w,o}} \tag{26}$$

The wet-bulb temperature is an important input. This is due to the fact that, at a given atmospheric pressure, enthalpy could be estimated using a formula that involves the wet-bulb temperature [44]. The mathematical manual of TRNSYS 18 describes more detailed mathematical formulas and references of open cooling towers [43]. In addition, prior studies have comprehensively validated the cooling tower model [43].

Based on the required cooling capacity, the air flow rate can be obtained. Ideally, the fan power increases cubically with the rotational speed (k = 3), as described in Equation (27) [45]. However, in this study, k is set to 1.5, reflecting practical in-situ operation data. In real-world operations, cooling towers do not achieve the ideal performance (k = 3) [45].

$$\frac{W_{ct}}{W_{ct,design}} = \left(\frac{Q_{ct}}{Q_{ct,design}}\right)^k \tag{27}$$

where, W_{ct} and $W_{ct,design}$ are the energy consumption of cooling towers and that at the design condition. Q_{ct} and $Q_{ct,design}$ are the air flow rate and that at the design condition.

The cooling tower fans' speed is adjusted to ensure that the outlet water temperature of the heat exchangers achieves 13 °C in the free cooling mode. The chiller controls the chilled water supply temperature in both partial free cooling mode and mechanical cooling mode. Meanwhile, the cooling tower fans' speed is regulated to ensure the outlet temperature of cooling towers at a setpoint determined by Equation (28). The control strategy of cooling towers is considered a near-optimal strategy [33].

$$T_{ct,out} = \max\left(T_{wet} + 5^\circ C, T_{\min,cd}\right) \tag{28}$$

where, $T_{ct,out}$ is the outlet temperature of cooling towers, T_{wet} is the wet bulb temperature, and $T_{min,ct}$ is the minimum setpoint of condenser water entering the temperature. As specified by the manufacturer, the water outlet temperature of the cooling tower must not fall below the minimum setpoint of condenser water entering temperature. Additionally, the cooling water return temperature is capped at 45 °C to prevent calcium salt precipitation [46].

3.3.3. Pump models

Variable-speed pumps are often selected for chilled water pumps for energy-saving purposes, whereas constant-speed pumps are often selected for cooling water pumps. The energy consumption of the chilled water pumps is calculated based on the water flow rate, the pressure drop of the loop and the efficiency of the chilled water pump, as described in Equation (29).

$$W_{cwp} = \frac{\Delta p_{cwp} \times m_w}{\eta_{cwp}} \tag{29}$$

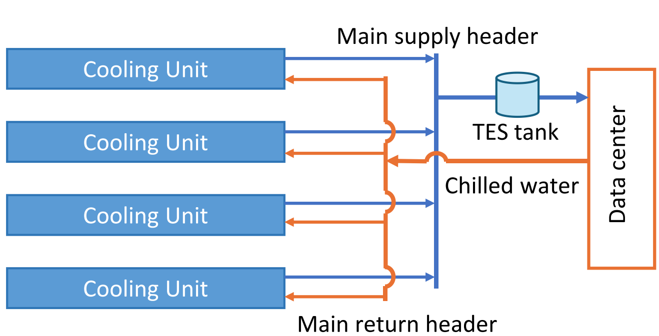

Fig. 5. Schematic of the cooling system in the referenced data center.

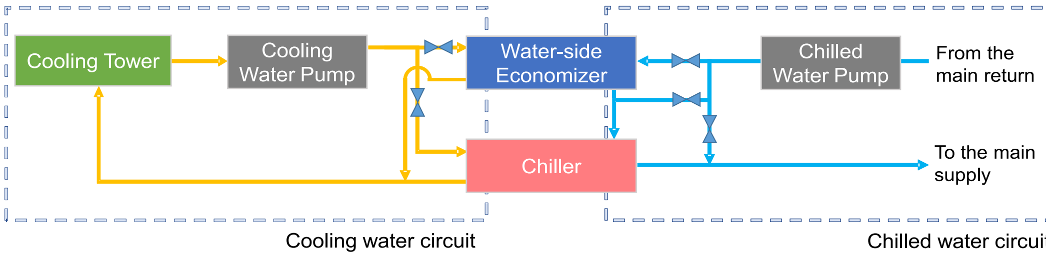

Fig. 6. Schematic of a cooling system unit.

Table 2
Specification of the cooling system in the referenced data center.

Cooling equipment	Number	Design specification
Chiller	4	Cooling capacity: 4200 kW Chilled water flow rate: 544300 kg/h Cooling water flow rate: 620000 kg/h
Heat exchanger	4	Heat transfer capacity: 4300 kW Water flow rate: 620000 kg/h
Chilled water pump (variable-speed)	4	Water flow rate: 620000 kg/h Pressure head: 500 kPa Power consumption: 110 kW
Cooling water pump (constant-speed)	4	Water flow rate: 620000 kg/h Pressure head: 350 kPa Power consumption: 84 kW
Cooling tower	4	Power consumption: 74 kW Heat rejection rate: 16800 kW
Electric heater	4	Power consumption: 60 kW

Table 3
The parameters associated with the chiller model.

Parameter	Value
a_0	0.4623
a_1	0.1659
a_2	0.1947
a_3	−0.3905
a_4	0.1469
a_5	0.4147
Q_{des}	4200 kW
ΔT_{des}	285 K
P_{des}	457.7 kW

The pressure head of pumps (equal to the pressure drop of the chilled water loop) is set to be linear to the water flow rate in operation [45] (Fig. 7). This control strategy is practically near-optimal and energy-efficient control of the chilled water loop. Additionally, the frequency of the chilled water pumps is regulated based on the required total water flow rate. To protect their motors, the speed of the chilled water pumps is limited to a range of 30 Hz–50 Hz.

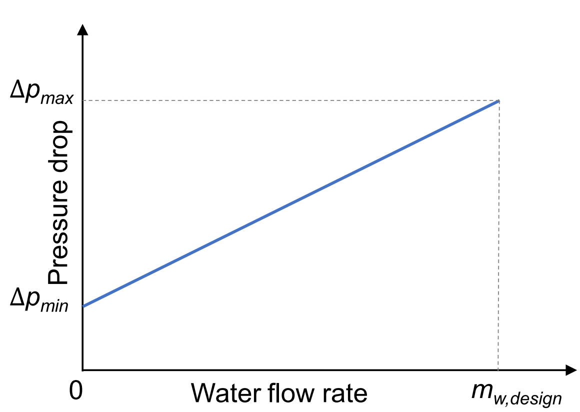

Fig. 7. Hydraulic characteristic of the chilled water loop.

4. Optimal dispatch strategy utilizing surplus capacity

The dispatch optimizations for both EES and TES are programmed in Python, with the optimization models solved using the Gurobi optimization solver. The dispatch optimization for EES is formulated as a mixed-integer linear programming problem. For the cooling system, the power consumption and cooling supply are represented as a piecewise-quadratic function based on regression analysis. The dispatch optimization for TES is addressed as a mixed-integer quadratic programming problem.

4.1. *Optimal dispatch strategy under the Guangdong electricity market in China*

Fig. 8A shows the Time of Use (ToU) electricity market in Guangdong Province, China, where electricity prices are categorized into peak, flat, and valley rates daily. Fig. 8B shows the optimized hourly dispatch results of electrical energy storage (EES), including charging/discharging as well as capacities provided for frequency regulation and spinning reserve. Fig. 8C shows the optimized hourly dispatch results of thermal energy storage (TES), including charging/discharging and the capacity provided for spinning reserve. The system charges during low-cost periods and discharges during high-cost periods, taking advantage of price differences to make a profit. Additionally, since providing frequency regulation services is more profitable than offering operating reserves, any extra capacity of the energy storage system is used for frequency regulation. Similarly, for Thermal Energy Storage (TES), charging takes place during periods of low tariffs, while discharging is timed with high tariffs to achieve energy arbitrage. In addition, TES is capable of providing reserve capacity as long as the stored energy in the TES tank remains above zero.

4.2. *Optimal dispatch strategy under the CAISO electricity market in the US*

Fig. 9A shows hourly energy, frequency regulation and spinning reserve prices of three typical days from the CAISO electricity market in the US. Fig. 9B shows the optimized hourly dispatch results of electrical energy storage (EES), including charging/discharging as well as capacities provided for frequency regulation and spinning reserve. It can be observed that the majority of surplus battery capacity is to provide frequency regulation service to generate revenue, with only a minor fraction being allocated for charging and discharging for energy arbitrage. This can be primarily attributed to the higher financial incentives associated with providing frequency regulation compared to those for operating reserve and energy arbitrage. Fig. 9C shows the optimized hourly dispatch results of thermal energy storage (TES), including charging/discharging and the capacity provided for spinning reserve. It

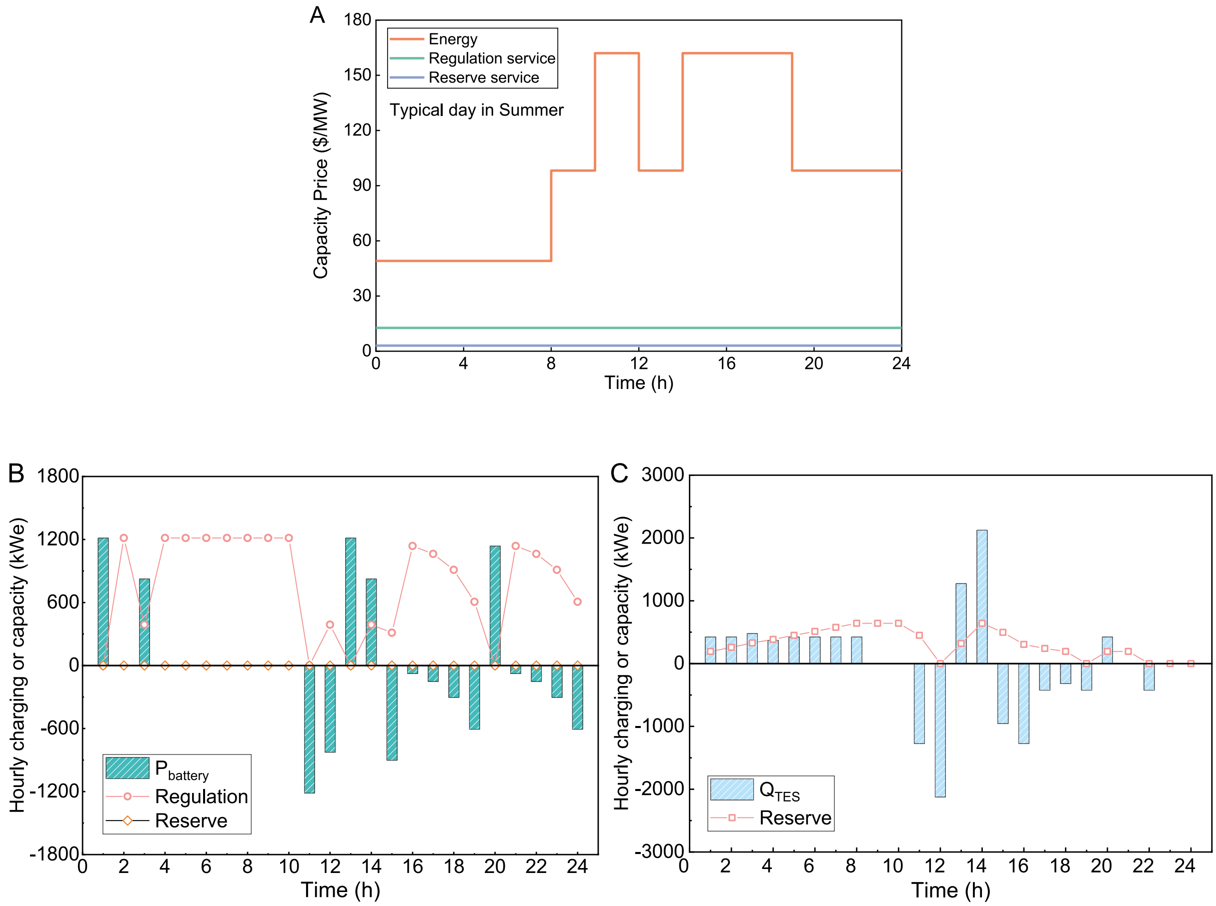

Fig. 8. (A) Time of Use (ToU) energy, regulation and operating reserve prices in Guangdong electricity market; (B) Optimal dispatch strategy of EES; (C) Optimal dispatch strategy of TES.

can be observed that the charging and discharging occur at low and high tariffs, respectively, thereby facilitating energy arbitrage. Similarly, TES can provide reserve service when the stored energy in the TES tank remains above zero.

5. Life-cycle economic benefits of design optimization under different electricity markets

5.1. Benefits under the Guangdong electricity market in China

Fig. 10A shows the life-cycle economic benefits of different scenarios of EES under the Guangdong electricity market. Due to multiple revenues from energy arbitrage and the provision of flexible services to the smart grid, the life-cycle economic benefits of Scenarios 1–4 all show better economic performance compared to the baseline scenario. Notably, the revenue from energy arbitrage accounts for a major portion, while the revenue from the provision of frequency regulation to the electricity market accounts for a minor portion under the Guangdong electricity market. Furthermore, Scenario 1 emerges as the most favorable, achieving higher profits ($-86,418) compared to the other scenarios (Scenario 1: the energy storage system for emergencies is a one-time investment and provides auxiliary services to the grid throughout the data center’s lifecycle). In addition, it can be observed that there are significant differences in capital costs across scenarios, primarily attributed to the discount rate and annual decline of battery price. This indicates that a staged investment results in a lower total investment amount when compared to a one-time investment.

Fig. 10B shows the life-cycle economic benefits of different scenarios of TES under the Guangdong electricity market. It can be observed that Scenario 1, Scenario 3 and Scenario 4 all yield positive profits over the lifetime, attributed to the revenues from energy arbitrage, the provision of reserve capacity and discount rates. Notably, Scenario 1 is still the most advantageous design option, yielding the highest profits, $205,213. This can be attributed to more revenue streams from energy arbitrage and the provision of reserve capacity to the grid. These revenue streams from the grid are higher than the economic benefits from a staged investment adopted in Scenarios 2–4.

5.2. Benefits under CAISO electricity market in the US

Fig. 11A shows the life-cycle economic benefits of different scenarios of EES under the CAISO electricity market. Unlike the results under the Guangdong electricity market, both Scenario 1 and Scenario 4 yield positive profits over the lifetimes under the CAISO electricity market. Similarly, Scenario 1 emerges as the most profitable design option for EES, yielding the highest economic benefit, $361,453. This indicates that the revenues from energy arbitrage and the provision of frequency regulation services to the grid are significantly higher compared to the Guangdong electricity market. Contrary to the results in the Guangdong electricity market, under the CAISO market, the majority of the revenue comes from providing frequency regulation services, while energy arbitrage contributes a smaller portion, which is significant from the results under the Guangdong electricity market. The reward associated with frequency regulation services under CAISO electricity market is significantly higher than under Guangdong electricity market.

Fig. 11B shows the life-cycle economic benefits of different scenarios of TES under the CAISO electricity market. Unlike the results under the Guangdong electricity market, only Scenario 1 yields a positive profit, of

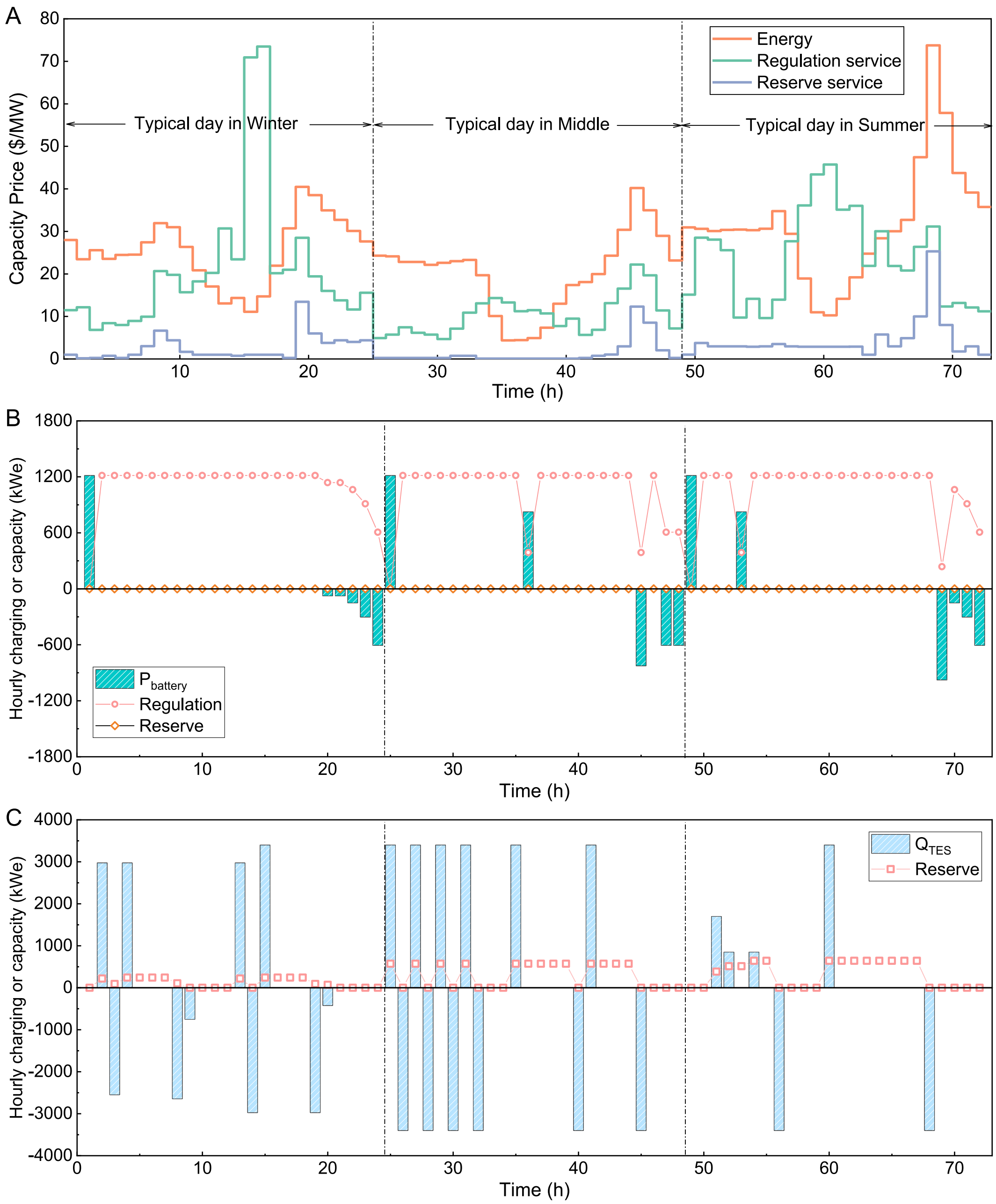

Fig. 9. (A) Hourly energy, frequency regulation and spinning reserve prices in 01/25, 04/25, and 09/27 from CAISO electricity market; (B) Optimal dispatch strategy of EES; (C) Optimal dispatch strategy of TES.

$36,98s5. This profitability is attributed to multiple revenue streams, including energy arbitrage and the provision of reserve capacity to the grid. Despite the presence of similar revenue streams in Scenarios 2–4, such as energy arbitrage, the provision of reserve capacity, and considerations of discount rates, these scenarios fail to achieve positive profits. The inability to generate positive profits in Scenarios 2–4 is primarily due to the fact that the revenue streams from the grid do not outweigh the economic benefits of a staged investment strategy implemented in these scenarios.

Overall, the results indicate that energy storage systems (EES) designed for emergencies can yield positive profits through participation in grid interactions. Under both electricity markets, Scenario 1 emerges as the optimal design option for deploying EES and TES for emergency use in data centers.

6. Impacts of discount rate and battery price on life-cycle economic benefits

6.1. Life-cycle economic benefits of electrical energy storage

6.1.1. Under the Guangdong electricity market in China

When the discount rate is set at 4 % and the annual decline rate of battery price is 5 %, Scenario 1 is identified as the optimal design option for deploying Energy Storage Systems (EES) and Thermal Energy Storage (TES) for emergency use in data centers. However, the results might be significantly different when these two critical factors vary.

Fig. 12 illustrates the impacts of discount rate and annual decline rate of battery price on the life-cycle economic benefits of four design scenarios under the Guangdong electricity market. It can be observed that both Scenario 2 (Fig. 12B) and Scenario 3 (Fig. 12C) do not exhibit economic benefits across a range of discount rates (2%–10 %) and

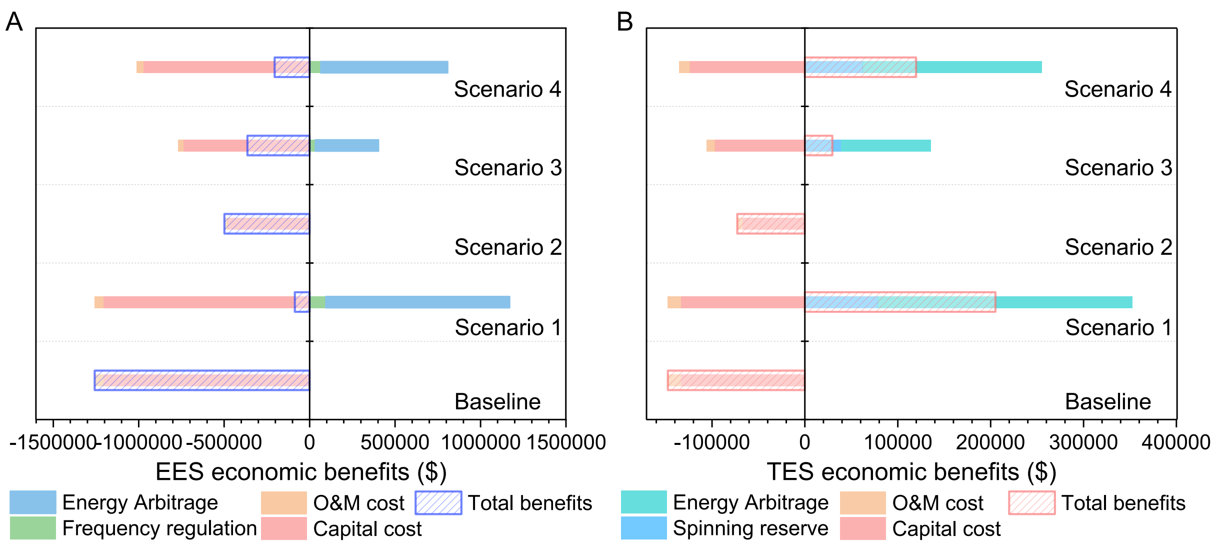

Fig. 10. Life-cycle economic benefits of different scenarios of (A) EES, (B) TES under the Guangdong electricity market, China.

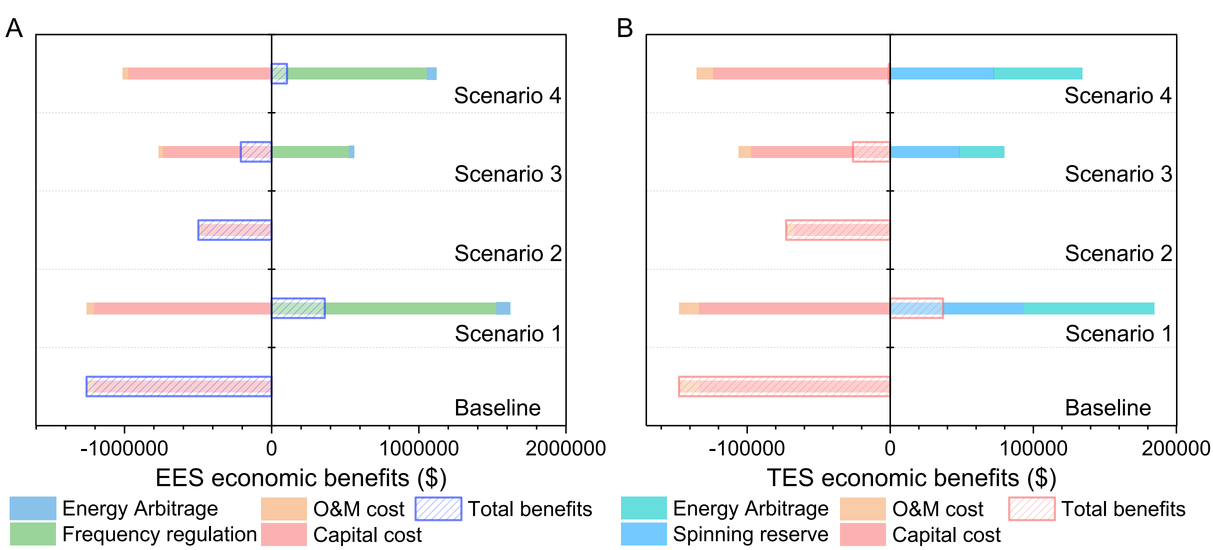

Fig. 11. Life-cycle economic benefits of different scenarios of (A) EES, (B) TES under CAISO electricity market.

battery price decline rates (5%–15 %). For Scenario 1, profits become positive when the discount rate falls below 2.7 % (Fig. 12A). Similarly, there is also a dividing curve for Scenario 4. In the lower right of the dividing curve in Fig. 12D (the discount rate of 9.5 % and the annual decline rate of battery price of 5.6 %), there are positive economic benefits. Generally, staged investments accompanied by revenues from grid services are more likely to yield positive returns with lower discount rates and higher annual decline rates of battery price.

6.1.2. *Under CAISO electricity market in the US*

Fig. 13 illustrates the impacts of discount rate and annual decline rate of battery price on the life-cycle economic benefits of four design scenarios under the CAISO electricity market. It can be observed that Scenarios 1, 3 and 4 each show dividing lines/curves where positive and negative economic benefits are represented on either side of the line/curve. For Scenario 1, profits are positive when the discount rate is less than 9 % (Fig. 12A). For Scenario 3 (Fig. 13C) and Scenario 4 (Fig. 13D), there are positive economic benefits in the lower right of the dividing curves. In addition, similar to the results under the Guangdong electricity market, Scenario 2 (Fig. 13B) does not exhibit economic benefits across a range of discount rates (2%–10 %) and battery price decline rates (5%–15 %).

6.2. *Impacts of discount rate on life-cycle economic benefits of thermal energy storage*

Fig. 14 shows the impact of the discount rate on the life-cycle economic benefits of TES under the Guangdong electricity market. It can be observed that Scenarios 1, 3 and 4 all exhibit positive economic benefits, which decrease as the discount rate increases from 2 % to 10 %. This trend can be attributed to the fact that a higher discount rate devalues future money, resulting in lower present values of future earnings. In contrast, Scenario 2 shows opposite results, exhibiting negative economic benefits and an uptrend as the discount rate increases. In Scenario 2, the energy storage system is designed for emergencies with a staged investment aligned with progressive IT loading, without providing additional dispatchable capacity for auxiliary services to the grid. As a result, future investments, when discounted back to their present value,

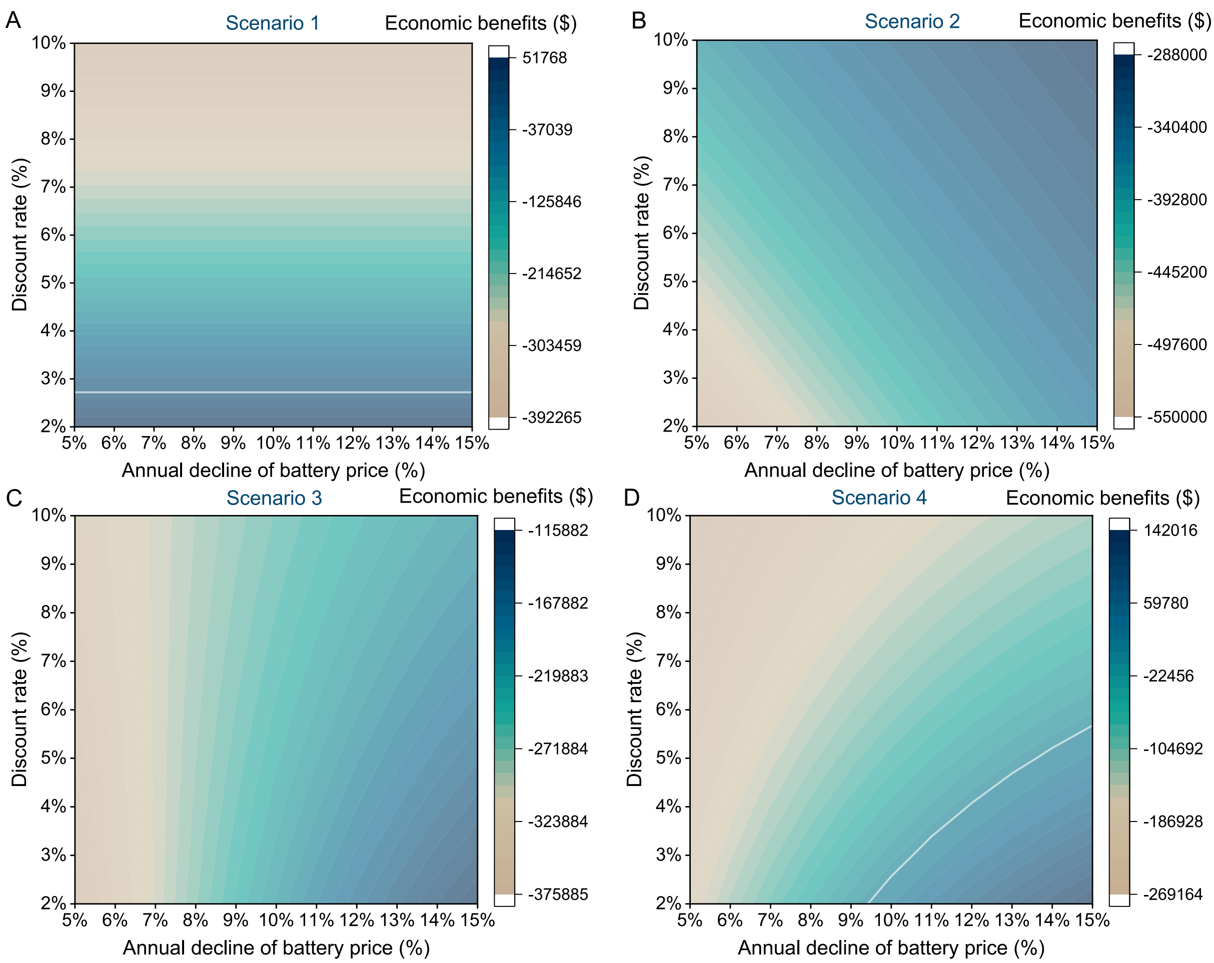

Fig. 12. Life-cycle economic benefits of EES versus discount rates and battery price decline rates under the Guangdong electricity market.

are less when the discount rate is higher.

Fig. 15 shows the impact of the discount rate on the life-cycle economic benefits of TES under the CAISO electricity market. It can be observed that only Scenario 1 shows positive economic benefits, and this is limited to instances where the discount rate is below 9 %. In this scenario, the economic benefits decrease as the discount rate increases from 2 % to 10 %. This can be attributed to the fact that a higher discount rate devalues future money and results in a lower present value of future earnings.

The other scenarios all show negative economic benefits across a range of discount rates (2%–10 %). For Scenario 2, the trend of economic benefits as the discount rate increases is similar to that under the Guangdong electricity market. However, in Scenarios 3 and 4, there is a noticeable decline in economic benefits as the discount rate rises from 2 % to 10 %. Both scenarios involve staged investments and revenues generated from providing services to the grid. As the discount rate increases, the present value of future earnings decreases more significantly, resulting in a downward trend.

7. Conclusions and discussion

This pioneering study focuses on the optimal dispatch and design of energy storage systems in data centers, particularly in the context of progressive IT loading. The main findings of this study are as follows.

Under both the Guangdong electricity market and the CAISO electricity market, the charging and discharging occur at low and high tariffs, respectively, thereby facilitating energy arbitrage. Furthermore, under the CAISO electricity market, a significant portion of the surplus battery capacity is allocated to provide frequency regulation services. In contrast, under the Guangdong electricity market, the majority of the surplus battery capacity is dedicated to energy arbitrage.

Under both electricity markets, Scenario 1 emerges as the optimal option with the highest life-cycle economic benefits. Specifically, under the Guangdong electricity market, the life-cycle economic benefits of EES and TES are $-86,418 and $205,213, respectively. Under CAISO electricity market, the life-cycle economic benefits of EES and TES are $361,453 and $36,985, respectively. Notably, the results reveal that EES yields greater economic benefits under the CAISO market, while TES yields greater economic benefits under the Guangdong market.

However, the results might be significantly different when the discount rate and annual decline rate of battery price vary. Typically, staged investments accompanied by revenues from grid services are more likely to yield positive returns with lower discount rates and higher annual decline rates of battery price. These results can be elucidated by examining the present value of future cash flows; as the discount rate escalates, the present value of both future earnings and investments correspondingly decreases.

In addition, for different types of growth patterns of IT load in data centers during lifetime, the method of optimal dispatch and investment scenarios are still suitable for practical implementation. However, care needs to be taken to survey the actual IT load factor carefully and ensure the basic functionality of the emergency energy storage system first. If there is excess capacity, it can be used to participate in grid response services.

The results provide valuable insights into the optimal dispatch and design of energy storage systems in data centers and guide the

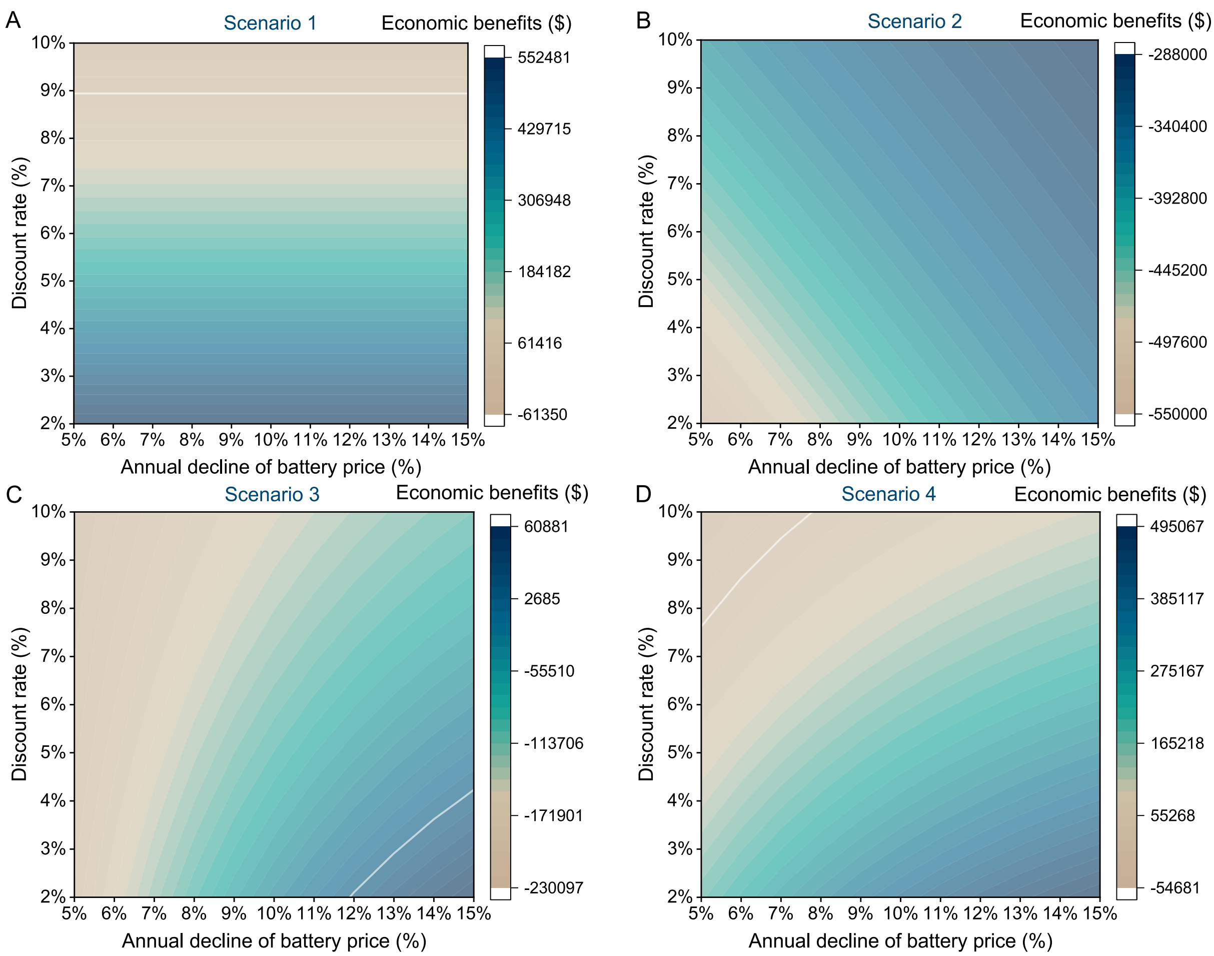

Fig. 13. Life-cycle economic benefits of EES versus discount rates and battery price decline rates under the CAISO electricity market.

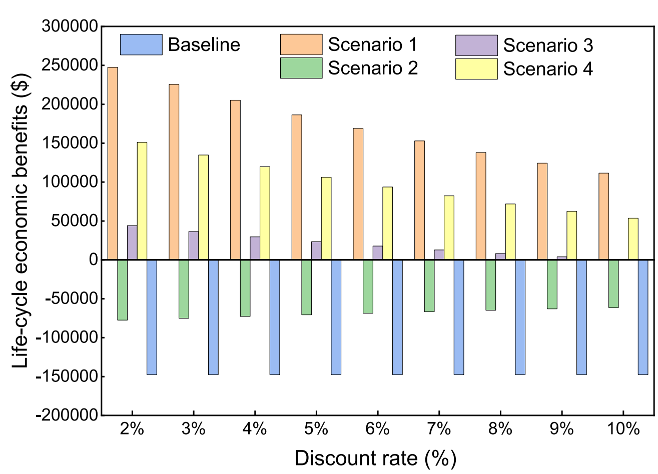

Fig. 14. Life-cycle economic benefits of TES under the Guangdong electricity market at discount ranging from 2 % to 10 %.

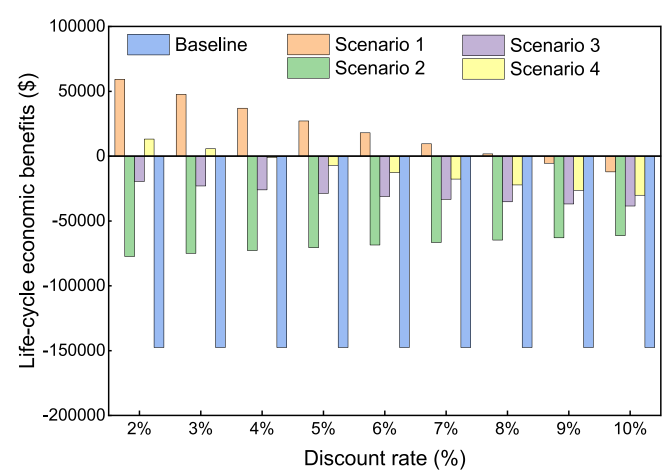

Fig. 15. Life-cycle economic benefits of TES under the CAISO electricity market at discount ranging from 2 % to 10 %.

development of next-generation data centers that can engage in dynamic interactions with energy systems. Data centers have the potential to play a significant role in the future energy landscape by actively participating in grid interactions and supporting the transition to a more sustainable and resilient power system.

CRediT authorship contribution statement

Yingbo Zhang: Writing – review & editing, Writing – original draft, Validation, Methodology, Investigation, Conceptualization. **Hong Tang:** Writing – review & editing, Investigation, Data curation. **Hangxin Li:** Supervision. **Shengwei Wang:** Writing – review & editing, Supervision, Funding acquisition, Formal analysis.

Declaration of competing interest

The authors declare that they have no known competing financial interests or personal relationships that could have appeared to influence the work reported in this paper.

Acknowledgment

The research of this paper is financially supported by a collaborative research fund (C5018-20G) and a grant under the Hong Kong PhD Fellowship Scheme of the Research Grants Council in the Hong Kong SAR.

Data availability

The authors do not have permission to share data.

References

[1] Zhang Y, Li H, Wang S. The global energy impact of raising the space temperature for high-temperature data centers. Cell Rep Phys Sci 2023;4(10).
[2] Masanet E, Shehabi A, Lei N, Smith S, Koomey J. Recalibrating global data center energy-use estimates. Science 2020;367(6481):984.
[3] Liu X, Shen C, Wang J, Zhang C, Shuai Y. Static and dynamic regulations of photovoltaic double skin facades towards building sustainability: a review. Renew Sustain Energy Rev 2023;183:113458.
[4] Liu X, Shen C, Yang H, Wang J. Comprehensive investigation on lighting and energy-saving performance of lighting/heating coupled tubular daylighting devices integrated with nanofluids. Appl Therm Eng 2024;239:122094.
[5] Wei W, Feng Z, Sun Y, Wang W, Jin X, Zhang J, et al. Experimental investigation on the space heating performance of air source heat pump with vapor injection under frosting condition. J Build Eng 2024;90:109327.
[6] Pu J, Xu D, Shen C, Lu L. Broadband-spectrally selective polymeric film for building integrated photovoltaic (BIPV) skylights cooling. Energy Convers Manag 2025;326:119453.
[7] He W, Xu Q, Liu S, Wang T, Wang F, Wu X, et al. Analysis on data center power supply system based on multiple renewable power configurations and multi-objective optimization. Renew Energy 2024;222:119865.
[8] Han O, Ding T, Zhang X, Mu C, He X, Zhang H, et al. A shared energy storage business model for data center clusters considering renewable energy uncertainties. Renew Energy 2023;202:1273–90.
[9] Zhou Z, Liu F, Chen S, Li Z. A truthful and efficient incentive mechanism for demand response in green datacenters. IEEE Trans Parallel Distr Syst 2018;31(1):1–15.
[10] Wang S, Qian Z, Yuan J, You I. A DVFS based energy-efficient tasks scheduling in a data center. IEEE Access 2017;5:13090–102.
[11] Kontorinis V, Zhang LE, Aksanli B, Sampson J, Homayoun H, Pettis E, et al. Managing distributed ups energy for effective power capping in data centers. Comput Architect News 2012;40(3):488–99.
[12] Chen H, Caramanis MC, Coskun AK Reducing the data center electricity costs through participation in smart grid programs. Conference Reducing the data center electricity costs through participation in smart grid programs. p. 1-10.
[13] Zhang Y, Wilson DC, Paschalidis IC, Coskun AK A data center demand response policy for real-world workload scenarios in HPC. Conference A data center demand response policy for real-world workload scenarios in HPC. IEEE, p. 282-287.
[14] Hu H, Wen Y, Yin L, Qiu L, Niyato D. Coordinating workload scheduling of geo-distributed data centers and electricity generation of smart grid. IEEE Trans Serv Comput 2020;13(6):1007–20.
[15] ASHRAE. Thermal guidelines for data processing environments. fifth ed. 2021.
[16] Ghatikar G. Demand response opportunities and enabling technologies for data centers: Findings from field studies. 2012.
[17] Fu Y, Han X, Baker K, Zuo W. Assessments of data centers for provision of frequency regulation. Appl Energy 2020;277:115621.
[18] Mares K. Demand response and open automated demand response opportunities for data centers. 2009.
[19] Zhang Y, Wang Y, Wang X. TEStore: exploiting thermal and energy storage to cut the electricity bill for datacenter cooling. Conference TEStore: exploiting thermal and energy storage to cut the electricity bill for datacenter cooling. IEEE, p. 19-27.
[20] Yang T, Zhao Y, Pen H, Wang Z. Data center holistic demand response algorithm to smooth microgrid tie-line power fluctuation. Appl Energy 2018;231:277–87.
[21] Guo C, Luo F, Cai Z, Dong ZY, Zhang R. Integrated planning of internet data centers and battery energy storage systems in smart grids. Appl Energy 2021;281:116093.
[22] Ma X, Zhang Q, Zou S. An experimental and numerical study on the thermal performance of a loop thermosyphon integrated with latent thermal energy storage for emergency cooling in a data center. Energy 2022;253:123946.
[23] Brett Griffin PE. Data center economizer efficiency. ASHRAE J 2015.
[24] Lyu W, Wang Z, Li X, Xin X, Chen S, Yang Y, et al. Energy efficiency and economic analysis of utilizing magnetic bearing chillers for the cooling of data centers. J Build Eng 2022;48:103920.
[25] Rasmussen N. Avoiding costs from oversizing data center and network room infrastructure. Whitepaper 2011;37:1–9.
[26] http://oasis.caiso.com/mrioasis/logon.do.
[27] Celebi E, Fuller JD. Time-of-use pricing in electricity markets under different market structures. IEEE Trans Power Syst 2012;27(3):1170–81.
[28] https://www.shanwei.gov.cn/swdpb/zxgk/201911/92c15ae1ab904fbfb7e93b8fd19b1694/files/85460ce1f31146acb019e23e6442f644.pdf.
[29] http://120.31.132.37:16001/portal-oa/unauth/readPdf?filePath=/biz/DOC_SEND/888.pdf.
[30] Shi Y, Xu B, Wang D, Zhang B. Using battery storage for peak shaving and frequency regulation: joint optimization for superlinear gains. IEEE Trans Power Syst 2017;33(3):2882–94.
[31] Tang H, Wang S. Life-cycle economic analysis of thermal energy storage, new and second-life batteries in buildings for providing multiple flexibility services in electricity markets. Energy 2023;264:126270.
[32] Tang H, Wang S. A model-based predictive dispatch strategy for unlocking and optimizing the building energy flexibilities of multiple resources in electricity markets of multiple services. Appl Energy 2022;305:117889.
[33] Cheung H, Wang S. Optimal design of data center cooling systems concerning multi-chiller system configuration and component selection for energy-efficient operation and maximized free-cooling. Renew Energy 2019;143:1717–31.
[34] Luerssen C, Gandhi O, Reindl T, Sekhar C, Cheong D. Life cycle cost analysis (LCCA) of PV-powered cooling systems with thermal energy and battery storage for off-grid applications. Appl Energy 2020;273:115145.
[35] Marczinkowski HM, Østergaard PA. Evaluation of electricity storage versus thermal storage as part of two different energy planning approaches for the islands Samsø and Orkney. Energy 2019;175:505–14.
[36] Li F, Sun B, Zhang C, Liu C. A hybrid optimization-based scheduling strategy for combined cooling, heating, and power system with thermal energy storage. Energy 2019;188:115948.
[37] Mauler L, Duffner F, Zeier WG, Leker J. Battery cost forecasting: a review of methods and results with an outlook to 2050. Energy Environ Sci 2021;14(9):4712–39.
[38] He G, Chen Q, Kang C, Pinson P, Xia Q. Optimal bidding strategy of battery storage in power markets considering performance-based regulation and battery cycle life. IEEE Trans Smart Grid 2015;7(5):2359–67.
[39] Kumbaroğlu G, Madlener R. Evaluation of economically optimal retrofit investment options for energy savings in buildings. Energy Build 2012;49:327–34.
[40] Braun JE. Methodologies for the design and control of central cooling plants. The University of Wisconsin-Madison; 1988.
[41] Lui YY. Waterside and airside economizers design considerations for data center facilities. Build Eng 2010;116(1):98–108.
[42] Taylor ST. How to design & control waterside economizers. ASHRAE J 2014;56(6):30–6.
[43] TRNSYS 18, A transient systems simulation program http://sel.me.wisc.edu/trnsys.
[44] Ma Z, Wang S, Xu X, Xiao F. A supervisory control strategy for building cooling water systems for practical and real time applications. Energy Convers Manag 2008;49(8):2324–36.
[45] Lu Y, Wang S, Zhao Y, Yan C. Renewable energy system optimization of low/zero energy buildings using single-objective and multi-objective optimization methods. Energy Build 2015;89:61–75.
[46] Pontes RFF, Yamauchi WM, Silva EKG. Analysis of the effect of seasonal climate changes on cooling tower efficiency, and strategies for reducing cooling tower power consumption. Appl Therm Eng 2019;161:114148.